College of Engineering

Comparison of Turbulence Models with use of UnTRIM in the Delaware Bay

Kutay Celebioglu[1], Michael Piasecki[2]

Abstract

In this paper, various turbulence closure models are compared for use with a hydrodynamic 3D code in the Delaware Bay. More specifically, six (6) different turbulence closures, i.e. a constant eddy viscosity, an algebraic model, and 4 two-equation closure models have been used for comparison. These models have been implemented in the UnTRIM hydrodynamic code using the Generic Length Scale approach that mimics through its parameter combinations 3 of the two-equation closures (k-ε, k-ω, and k-kl) plus a separate Yamada Mellor 2.5 code. The UnTRIM code was used to model flows and salinity transport for a 2 month period by keeping the boundary and initial conditions unchanged for all model comparisons. The performance of each closure scheme was tested against salinity time series at a single station in the estuary. The comparisons reveal that the zero and first order approaches perform fair, but less accurate than the two-equation models that warrants the increased computational cost associated with these higher order approaches. Among the four 2-equation models, the k-ε model best represented the measured salinity time histories in the bay. The differences when compared to the other 2-equation models were significant enough to conclude that an arbitrary choice from the list of available or commonly used turbulence closure models is not sufficient. As a result, it is recommended that a test series be conducted to identify the best choice of turbulence closure in a specific application.

1. Introduction

The Delaware Bay extends from Cape May (NJ) and Cape Henlopen (DE) to its head of tide boundary at Trenton (NJ). The Bay is approximately 215 km in length and has a navigational channel of 12 m depth throughout its extent. The navigational channel covers most of the width in the upper portion of the estuary, which is between river kilometers 100 to 215. The estuary is nearly 18 km wide at its mouth (river kilometer 0), with the width reaching its largest extend of 42 km almost 20 km upstream of the mouth.

A numerical 3D model for the tidal portion of the Delaware Bay has been developed using the UnTRIM hydrodynamic kernel (Casulli and Walters 2000; Casulli and Zanolli 2002). The model extends from Trenton, NJ south past the inlet at Cape May, NJ and incorporates a large portion of the continental shelf (up to the 50 meter

[1] Research Assist., Dept. of Civil, Architectural & Environ. Engr., Drexel University, Philadelphia, PA 19104; Kutay@drexel.edu
[2] Assoc. Prof., Dept. of Civil, Architectural & Environ. Engr., Drexel University, Philadelphia, PA 19104; Michael.Piasecki@drexel.edu

isobath) to capture the processes of the continental shelf and their relation and impact on the bay dynamics.

Sediment properties and dynamics in the Delaware Bay show large disparity throughout the bay. In a recent work, Sommerfield and Madsen (2003) developed an interpretable map of bottom sediment types of the estuary between Burlington, New Jersey and New Castle, Delaware. They also quantified recent sedimentation rates using the chronologies developed from profiles of an artificial radioisotope. Of particular importance is the location of the turbidity maximum that has been shown to migrate between river kilometers 75 and 120 (Cook 2004), indicating a considerable variation in the location and intensity of turbidity maximum.

The proper choice of a turbulence model is of utmost importance if one is ever to succeed in modeling the fate and transport of dissolved or particulate constituents. While turbulent mixing occurs in all three directions, horizontal mixing terms are at least two orders of magnitudes smaller than the substantial derivative of the horizontal velocity components. In circulation models these terms are not resolved due to large grid spacing and parameterizations can be used (Burchard 2002 p.31). Consequently, the focus is on the vertical mixing for which a closure model must be found. Additionally, while the inclusion of a sediment transport model would be preferable in determining the performance of the turbulence closure (this would also better identify the location of the turbidity maximum), a conservative constituent (salinity) is used as a surrogate indicator. This is warranted as i) the salinity front typically aligns itself with the turbidity maximum, ii) salinity concentrations both in the vertical and horizontal directions react to different turbulence closure models.

Typically, it is not known a priori what level of complexity is necessary to adequately represent vertical turbulence closure. Choices range from a simple constant eddy viscosity/diffusivity, to an algebraic model to a number of more sophisticated two-equation models with an increasing demand on effort and computational resources (Large eddy simulation (LES) or direct numerical simulation (DNS) are not considered here because of the prohibitively large scale of the modeling domain). The questions posed are: what level complexity is needed? Is a constant eddy viscosity approach sufficient or do one need to deploy a two-equation closure model? In a second question one could then ask, which of the two-equation models performs best or do they all perform at the same level? To this end the Generic Length Scale (GLS) model (Umlauf and Burchard 2003) is implemented into the UnTRIM code to test various schemes and their performance given the specific settings in the Delaware Bay. In total, six variations; one constant eddy viscosity, an algebraic approach, and 4 two equation closures, i.e. Mellor-Yamada level 2.5, k-ε, k-ω, and k-kl parameterizations of GLS; are tested.

2. Numerical Model

The hydrodynamic system, being complex, requires a stable and efficient way of solving the governing equations. UnTRIM is a semi-implicit scheme for solving the hydrodynamic equations on specially arranged unstructured grids and shares the same philosophy with the family of TRIM models (Casulli 1990). The numerical model UnTRIM solves the Reynolds Averaged Navier-Stokes equations (RANS) together with a scalar transport equation (Casulli and Zanolli 2005) for salinity and temperature on an unstructured orthogonal grid. In this study, the hydrodynamics are modeled using model forcings such as the tidal water surface elevation at the open boundary, fresh water inflow at the tributaries, and meteorological conditions like wind fields.

2.1. Model Setup

The unstructured orthogonal grid for Delaware Bay was generated by the grid generator JANET (Sellerhoff and Lippert 2005). A horizontal grid that consists of 7445 quadrilateral and 2635 triangular polygons was produced (Figure 1). The size of the polygons ranges from 40m on the upstream boundary at Trenton to 2500m at the continental self. The grid has been designed by gradually changing the grid size and keeping the center of polygons nearly the same distance from the shared side, thus, minimizing the deviation from second order accuracy (Celebioglu and Piasecki 2004). The vertical grid spacing is set to 1m, and 1.25 million sounding values were extracted from the NOS (National Ocean Service) GEODAS-CD to provide a base for the bathymetry. These points were then triangulated to generate a digital terrain model (DTM) that is then used to calculate bathymetric depths at each edge of the polygon. The depth values are subsequently converted to mean sea level using the VDatum software tool (Hess 2002; Parker et al. 2003) which was developed jointly by NOAA's Office of Coast Survey and the National Geodetic Survey.

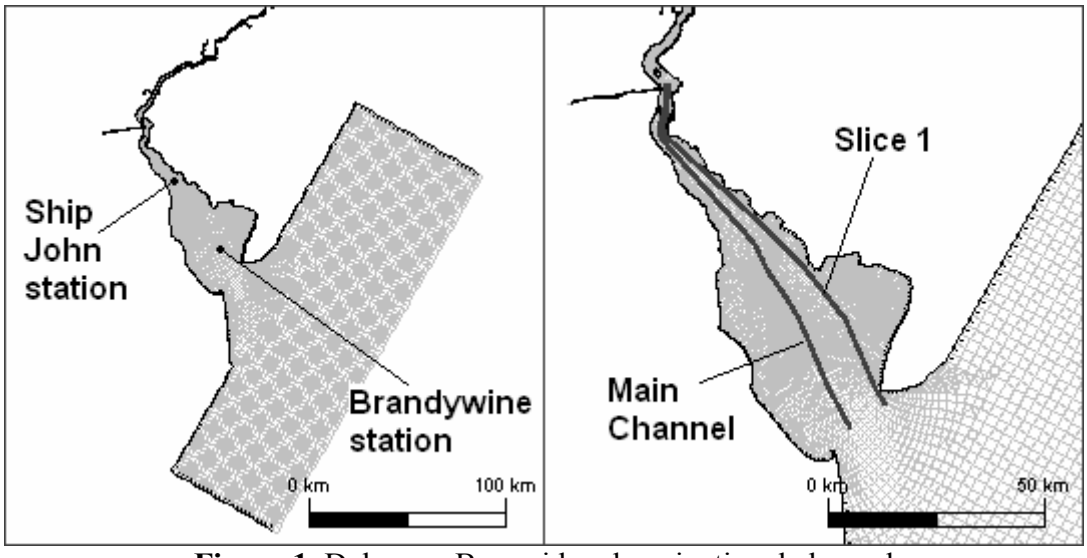

Figure 1. Delaware Bay grid and navigational channel

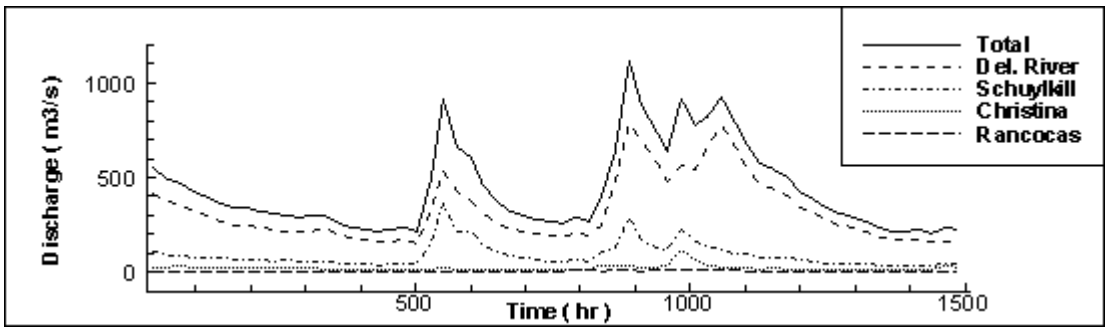

Figure 2. Freshwater inflow for July – August, 2003

The predominant constituent of the tidal signal in the bay is the M_2 tide. The effect of other astronomical tides such as O_1, K_1, N_2, S_2 and the effect of over tide M_4 are small compared to the M_2. These tides generate tidal currents with a typical speed of 1.0 m/s in the channel.

There is a considerable effect of forcing by the Chesapeake Bay through the C&D canal and the open boundary of the Delaware Bay. At semidiurnal tidal frequency, the barotropic response of Delaware estuary is predominantly driven by the forcing from the ocean through the mouth of the estuary. However, the volume exchange is strongly influenced by the Chesapeake Bay via the C&D canal at subtidal frequencies (Wong 1991). This influence changes not only the volumetric flow through the bay but also the response of the bay to the forcing at the mouth of the bay.

In order to simulate these effects, a variable, harmonically decomposed, water level boundary condition of three diurnal (K_1, Q_1, O_1) and four semi-diurnal (K_2, S_2, N_2, M_2) components in both space and time is extracted from the East Coast Tidal Database (Mukai et al. 2001). It is assumed that the extracted main components generate adequate open boundary conditions at the continental shelf boundary and that the nonlinear components are generated by the numerical model within the domain. The water level at the Chesapeake Bay end of C&D canal are calculated using the K_1, Q_1, O_1, K_2, S_2, N_2, M_2, and SA components from the NOAA/NOS station (ID: 8573927) at Chesapeake City, MD.

The Delaware River is a major the tributary of Delaware Bay, where the upstream dam at Trenton maintains a minimum flow of 85 m^3/s (regulated). There are several other tributaries flowing into the Delaware estuary, the largest of which is the Schuylkill River. The inflow from Schuylkill River accounts for 20% of the total fresh water inflow during the low flow periods in summer (Figure 2). The freshwater inflow values are obtained from USGS stations throughout the bay and the significant sources such as Delaware River, Schuylkill River, Christina River, and Rancocas River are used as boundary forcing.

A quadratic drag law is used at both bottom and surface boundaries. The bottom drag coefficient varies between 0.0025 and 0.0045 in order to best match the observed

tidal characteristics. A constant drag coefficient of 1.75×10^{-6} is used for the surface layer.

Uniform wind forcing over the entire domain is applied using the NOS buoy data (Figure 3). South, south-west winds are dominant except certain periods of time when strong north-east wind events are observed.

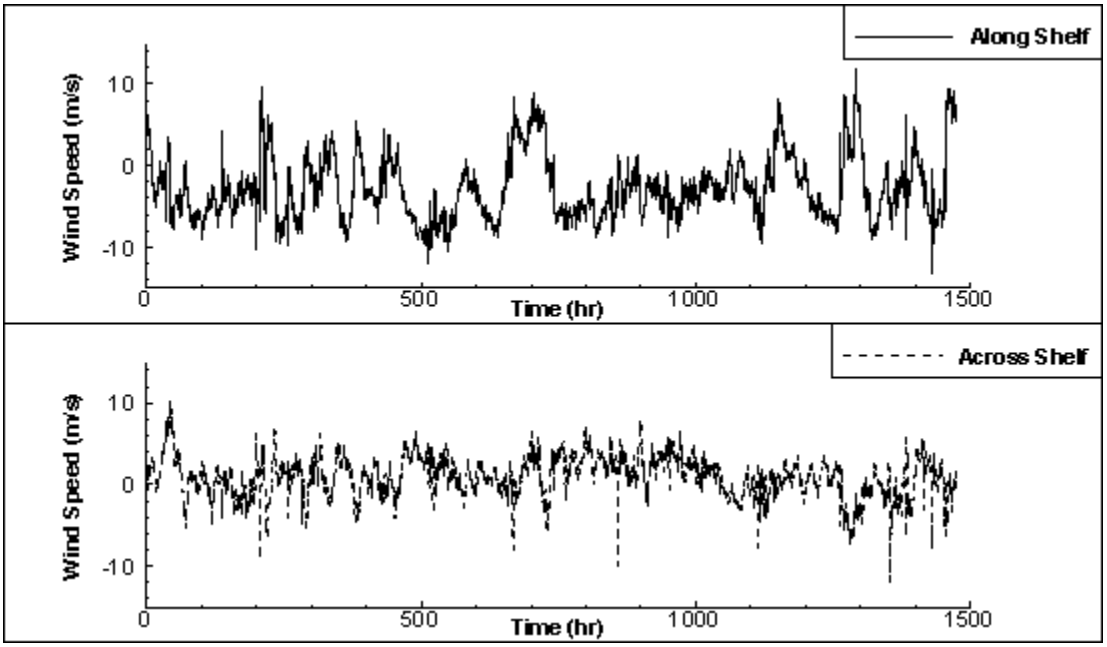

Figure 3. Along and across self wind forcing

The UnTRIM model uses a semi-implicit method, which incorporates an Eulerian-Lagrangian approximation for the advective terms, making the method unconditionally stable for barotropic flows (Casulli and Walters 2000). The numerical scheme is subject to a weak Courant-Friedrichs-Lewy (CFL) stability condition for internal waves (baroclinic flows). An estimate for time step based on the maximum internal wave speed can be calculated for the Delaware Bay. A grid size of 300m and salinity difference of 30 PSU (which introduces 21 kg/m^3 difference in density) yield:

$$\Delta t_{\max} \approx \frac{\Delta x}{\sqrt{g \frac{\Delta \rho}{\rho_0} h}} = \frac{300}{\sqrt{9.81 \times \frac{21}{1000} \times 15}} \approx 170 \sec$$

Although the model is stable at higher time step values, a time step of 150 seconds is used in the simulations. UnTRIM also allows wetting and drying of polygons which is crucial as significant portions of the estuary fall dry during ebb-tide.

2.2. Turbulence Models

The vertical and longitudinal distribution of salinity is an important aspect when modeling flows in the Delaware Bay, for one because the knowledge of the saline waters is of importance to the oyster fisheries but also because its distribution serves as a good indicator variable how different turbulence closure models behave. The Delaware Bay is a weakly stratified estuary (Garvine et al. 1992) because the ratio of the tidal excursion volume to the freshwater inflow is large. However, in the main channel stratification exists, which is particularly prominent during the onset of ebb and high tide. The salinity in the river is closely related to the freshwater inflow, which in turn, is strongly influenced by the rainfall patterns. These patterns are associated with large scale storm events which produce large seasonal and interannual variations in salinity. Wong (1995) suggested that the response of the vertical salinity structure to the change in river discharge results in a variation of longitudinal–salinity distribution with lateral variability which can be explained by density induced gravitational circulation.

In complex flows, lower order turbulence models become very cumbersome to use because they need to be fine-tuned locally. On the other side, 2-equation models are better suited to accurately represent the physics of turbulence and their influence both on the flow field and the transport of solutes and particulate matter. A class of 2-equation models for turbulence closure has been extensively applied to estuarine simulation. The most commonly used ones are the Mellor and Yamada (Mellor 1982), modeling the turbulent kinetic energy (k) and the length scale (l); k-ε model of Rodi (1987), modeling the turbulent kinetic energy (k) and its dissipation rate (ε) and the k-ω model of Wilcox (1988).

Recently Umlauf and Burchard (2003) proposed a generic length scale (GLS) equation that can represent the transport of l, ε and ω by a single equation. Application of this method enables the user to choose a variety of two equation methods. The ability to execute a code using the various closure methods prompted the use of the GLS because it permits a straightforward comparison between the closure approaches. Here, the GLS turbulence closure is implemented into UnTRIM model for the simulation of Delaware Bay.

2.3. Implementation of GLS Turbulence Closure to UnTRIM

The GLS model solves a transport equation for turbulent kinetic energy (k) and a transport equation for a generic parameter (ψ). The generic parameter is defined by:

$$\psi = \left(c_\mu^0\right)^p \cdot k^m \cdot l^n \tag{1}$$

Depending on the value of p, m and n (1) the parameter takes the form of different turbulent closure parameters like ε, w, l. The transport equation for (k) in a Cartesian coordinate system is given by:

$$\frac{\partial k}{\partial t}+\frac{\partial (uk)}{\partial x}+\frac{\partial (vk)}{\partial y}+\frac{\partial (wk)}{\partial z}=\frac{\partial}{\partial x}\left(\upsilon_H \frac{\partial k}{\partial x}\right)+\frac{\partial}{\partial y}\left(\upsilon_H \frac{\partial k}{\partial y}\right) + \frac{\partial}{\partial z}\left(\frac{K_M}{\sigma_k}\frac{\partial k}{\partial z}\right)+P+B-\varepsilon \tag{2}$$

Similarly the transport equation for the generic parameter (ψ) is given by:

$$\frac{\partial \psi}{\partial t}+\frac{\partial (u\psi)}{\partial x}+\frac{\partial (v\psi)}{\partial y}+\frac{\partial (w\psi)}{\partial z}=\frac{\partial}{\partial x}\left(\upsilon_H \frac{\partial \psi}{\partial x}\right)+\frac{\partial}{\partial y}\left(\upsilon_H \frac{\partial \psi}{\partial y}\right) + \frac{\partial}{\partial z}\left(\frac{K_M}{\sigma_\Psi}\frac{\partial \psi}{\partial z}\right)+\frac{\psi}{k}\left(c_1 P+c_3 B-c_2 \varepsilon F_{wall}\right) \tag{3}$$

To solve the above equations a fractional step method is used. In this approach, the advection and diffusion terms are time stepped using the UnTRIM transport scheme (Casulli and Zanolli 2005) after which the turbulent kinetic energy (k) and generic parameter (ψ) are updated using source and sink terms. While calculating and updating the sources and sinks, the calculation procedure of Warner et al (2005) is closely followed and identical values of the constants are used in (4) through (17). This procedure is explained in detail below.

After the advective and diffusive transport of turbulent kinetic energy (k) and generic parameter (ψ) using the UnTRIM engine, the values are interpolated into cell faces. The minimum values of k and Ψ are set. The values of velocity gradient (M) and buoyancy frequency (N^2) are calculated using:

$$M^2=\left[\left(\frac{\partial U}{\partial z}\right)^2+\left(\frac{\partial V}{\partial z}\right)^2\right] \tag{4}$$

$$N^2=-\frac{g}{\rho_0}\frac{\partial \rho}{\partial z} \tag{5}$$

An upper or lower limit depending on the value of n is imposed on ψ

$$\psi^{1/n} \le \sqrt{0.56}\left(c_\mu^0\right)^{p/n} k^{m/n+1/2} N^{-1} \tag{6}$$

Then the length scale is calculated using:

$$l=\left(c_\mu^0\right)^{-p/n} k^{-m/n} \psi^{1/n} \tag{7}$$

The eddy viscosity (K_M) and diffusivity (K_H) values are calculated using Kantha and Clayson (1994) type stability functions S_M and S_H:

$$S_H = \frac{a_2\left(1-6\,a_1/b_1\right)}{1-3a_2G_h\left(6a_1+b_2\left(1-c_3\right)\right)} \tag{8}$$

and

$$S_M = \frac{b_1^{-1/3}+\left(18a_1a_1+9a_1a_2\left(1-c_2\right)\right)S_HG_h}{1-9a_1a_2G_h} \tag{9}$$

Where $G_h = -\frac{N^2l^2}{2k}$ in (9) and an upper limit is imposed as

$$G_h^{\max} = \frac{1}{\mathrm{a}_2\left(\mathrm{b}_1+12.0\mathrm{a}_1+3\mathrm{b}_2\left(1\text{-}\mathrm{c}_3\right)\right)} \tag{10}$$

Then vertical turbulent viscosity and diffusivity is calculated from

$$K_M = c\cdot\sqrt{2k}\cdot l\cdot S_M+\upsilon \tag{11}$$

and

$$K_H = c\cdot\sqrt{2k}\cdot l\cdot S_H+\upsilon_\theta \tag{12}$$

Where υ and υ_θ are the molecular viscosity and diffusivity in (11) and (12) respectively. In the next step, the production (P) and buoyancy (B) of turbulent kinetic energy is calculated by:

$$P = K_M\cdot M^2 \tag{13}$$

$$B = -K_H\cdot N^2 \tag{14}$$

Where M^2 is given by (4) and N^2 is given by (5). The dissipation rate (ε) is calculated from:

$$\varepsilon = \left(c_\mu^0\right)^{3+(p/n)}\cdot k^{(3/2)+(m/n)}\cdot\psi^{-(1/n)} \tag{15}$$

The turbulent kinetic energy k and length scale parameter ψ is then updated using the fractional step method:

$$\frac{k^{new} - k^{UnTRIM}}{\Delta t} = P + B - \varepsilon \tag{16}$$

and

$$\frac{\psi^{new} - \psi^{UnTRIM}}{\Delta t} = \frac{\psi^{UnTRIM}}{k^{UnTRIM}}\left(c_1 P + c_3 B - c_2 \varepsilon F_{wall}\right) \tag{17}$$

2.4. Simulations

Six different turbulence closures are used for over a period of two months (July - August 2003) to capture varying flow conditions over medium-size duration. A constant eddy viscosity, mixing length theory with Richardson number modification, GLS formulation with *k-ε, k-ω and k-kl* parameterization and the original Mellor-Yamada level 2.5 (MY25) closure is used and compared with data.

The generality of the GLS model essentially allows for an infinite number of parameter combinations as selection of which could be tested as well. While this may seem an exercise akin to "curve-fitting", the objective was to compare those combinations that correspond to the most commonly known closure models.

3. Results

Seven major tidal constituents are used to reproduce water surface elevations, which are sufficiently accurate and are used as the tidal boundary conditions. In Figure 4 and Figure 5, water surface elevations of two NOAA stations, Ship John shoal light and Brandywine shoal light (Figure 1), are compared to UnTRIM simulations with GLS and MY25.

All of the models accurately represented the time series of water levels although the GLS formulation with *k-ε* parameterizations shows a slight underestimation of amplitudes compared to other models. None of the models are calibrated for tidal amplitudes using friction coefficients.

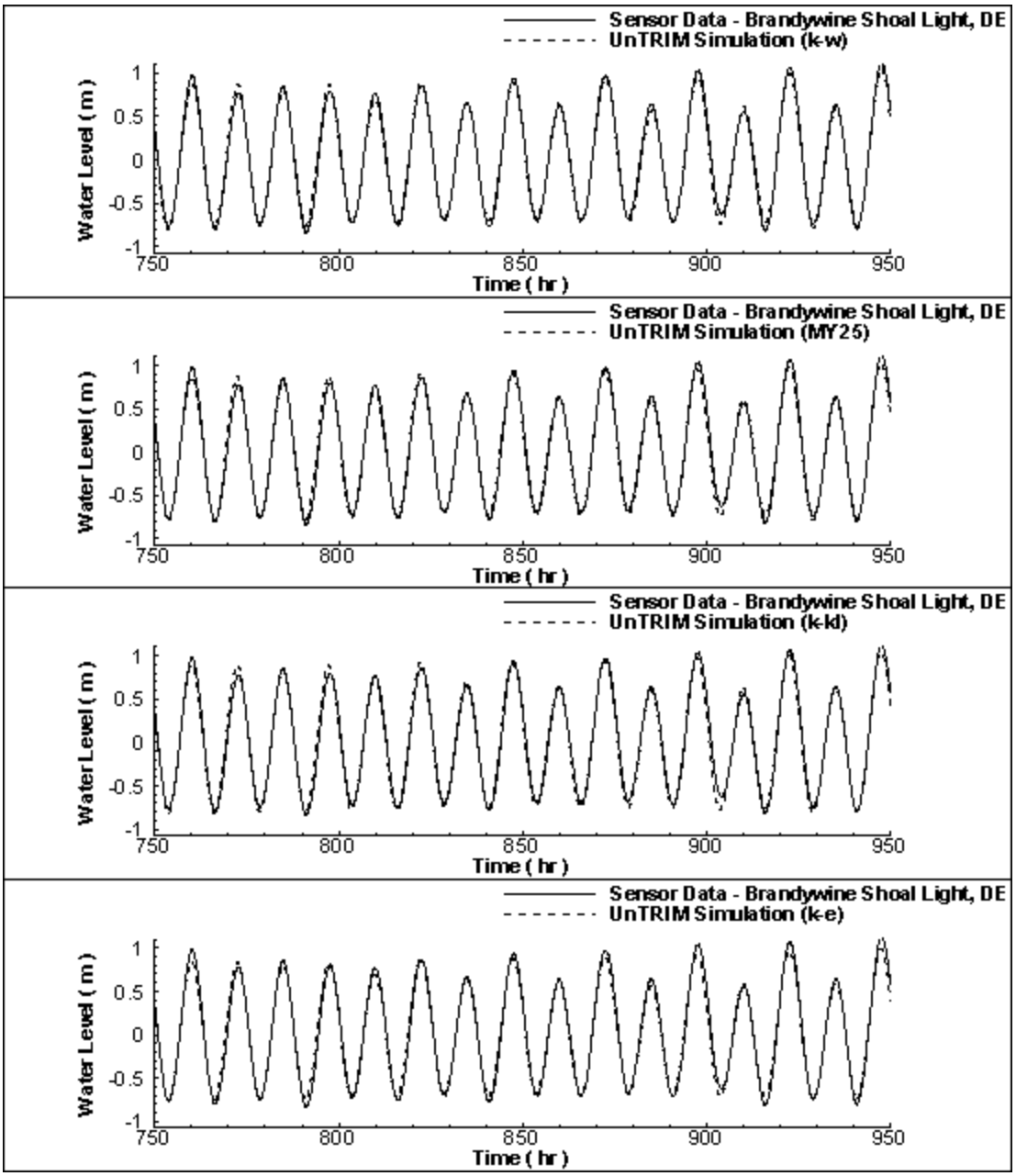

Figure 4. Comparison of simulated water levels to measured water level data for different turbulence closures at Brandywine Shoal Light, NJ

The comparison of salinity data at the Ship John station to UnTRIM simulations is shown in Figure 6. The variation in salinity amplitudes are not captured by the algebraic closure or the constant viscosity approach. Consequently, it appears that a more complex approach than the low order closures is needed to better characterize the nature of turbulence mixing. Throughout the simulation period, the k-ε model closely followed the salinity values. The MY25 closure and its representation k-kl in GLS present similar values for salinities. Although the same wall proximity functions are used in the model, minor differences in amplitudes are observed. The reason is the additional limitations implemented in GLS model given by (6).

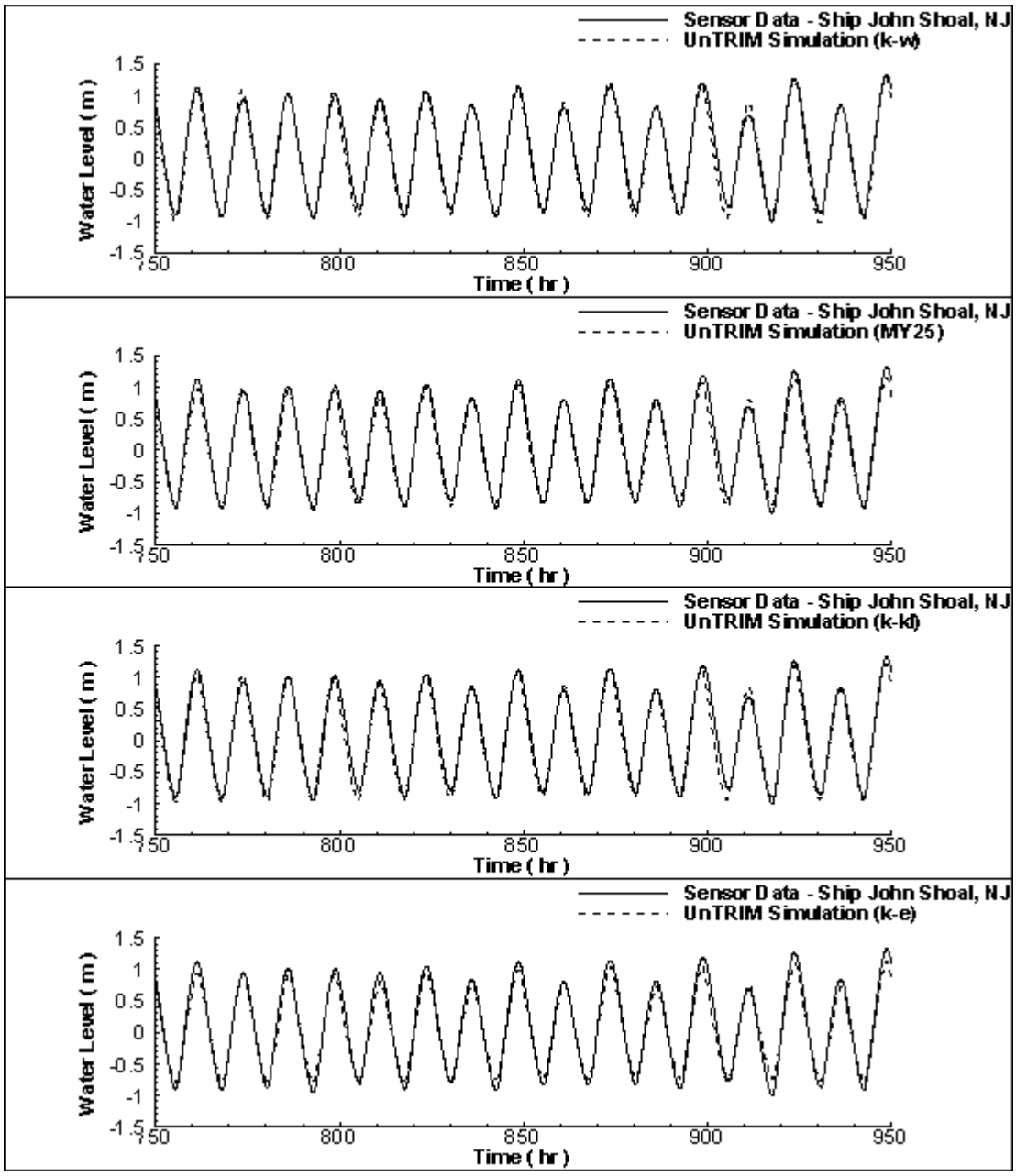

Figure 5. Comparison of simulated water levels to measured water level data for different turbulence closures at Ship John Shoal Light, NJ

In the *k-ω* model the amplitudes of fluctuations are overestimated. In addition, the *k-ω* predicts a greater degree of salinity intrusion (an additional 13 km) than the other models. Consequently, the mean salinity values at the Ship John station deviate substantially from the data. The response to the wind events at 600hrs present similar increasing and decreasing trends in both *k-ω, k-kl* and MY25 models (Figure 6).

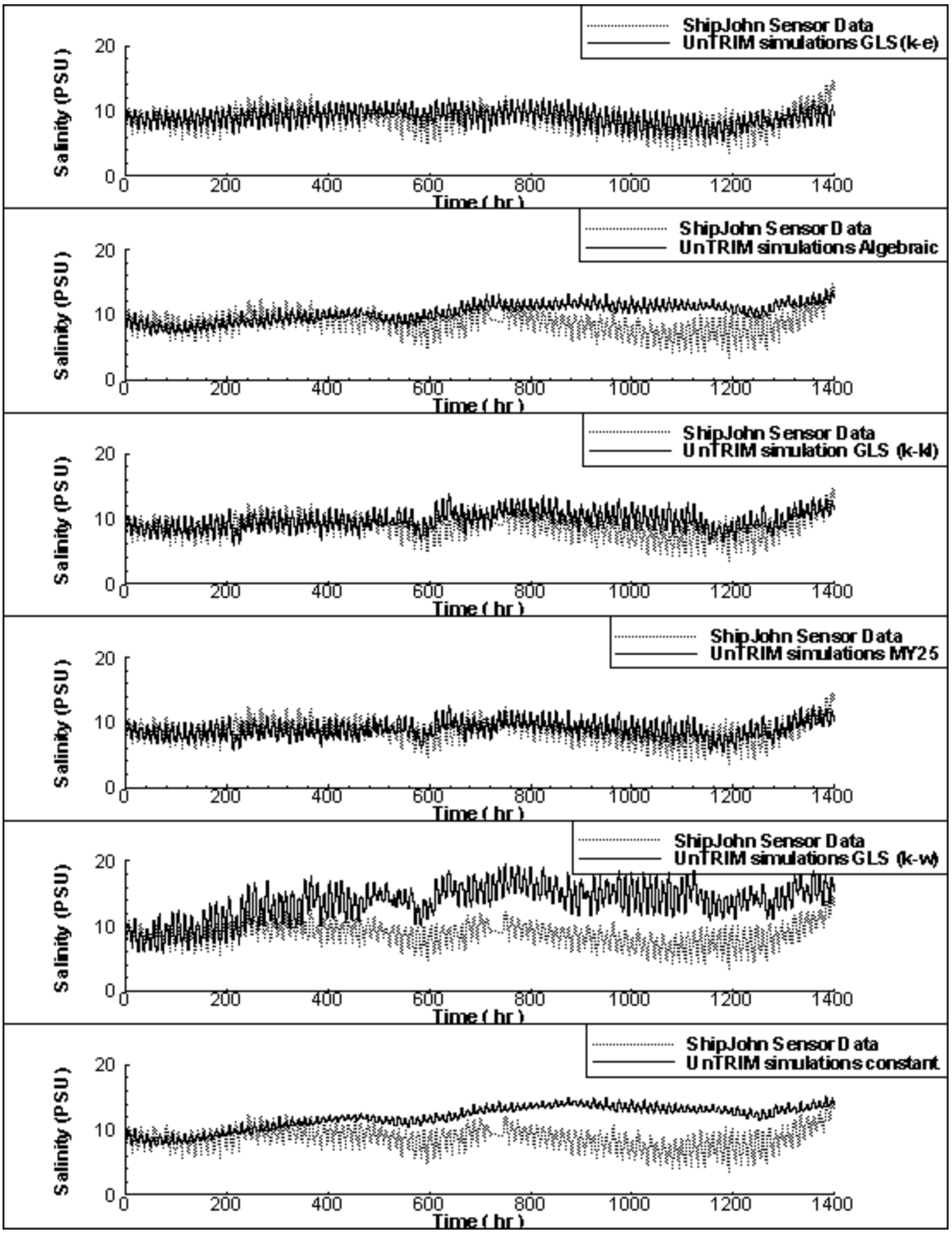

Figure 6. Comparison of simulation salinity variations to measured salinity for different turbulence closures.

In order to better demonstrate the differences in salinity stratification, two longitudinal cross-sections are identified, one is the main navigational channel and the other (slice 1) a shallower section (Figure 1). Snapshots of vertical profiles along the main channel are plotted for ebb (Figure 7) and flood tides (Figure 8).

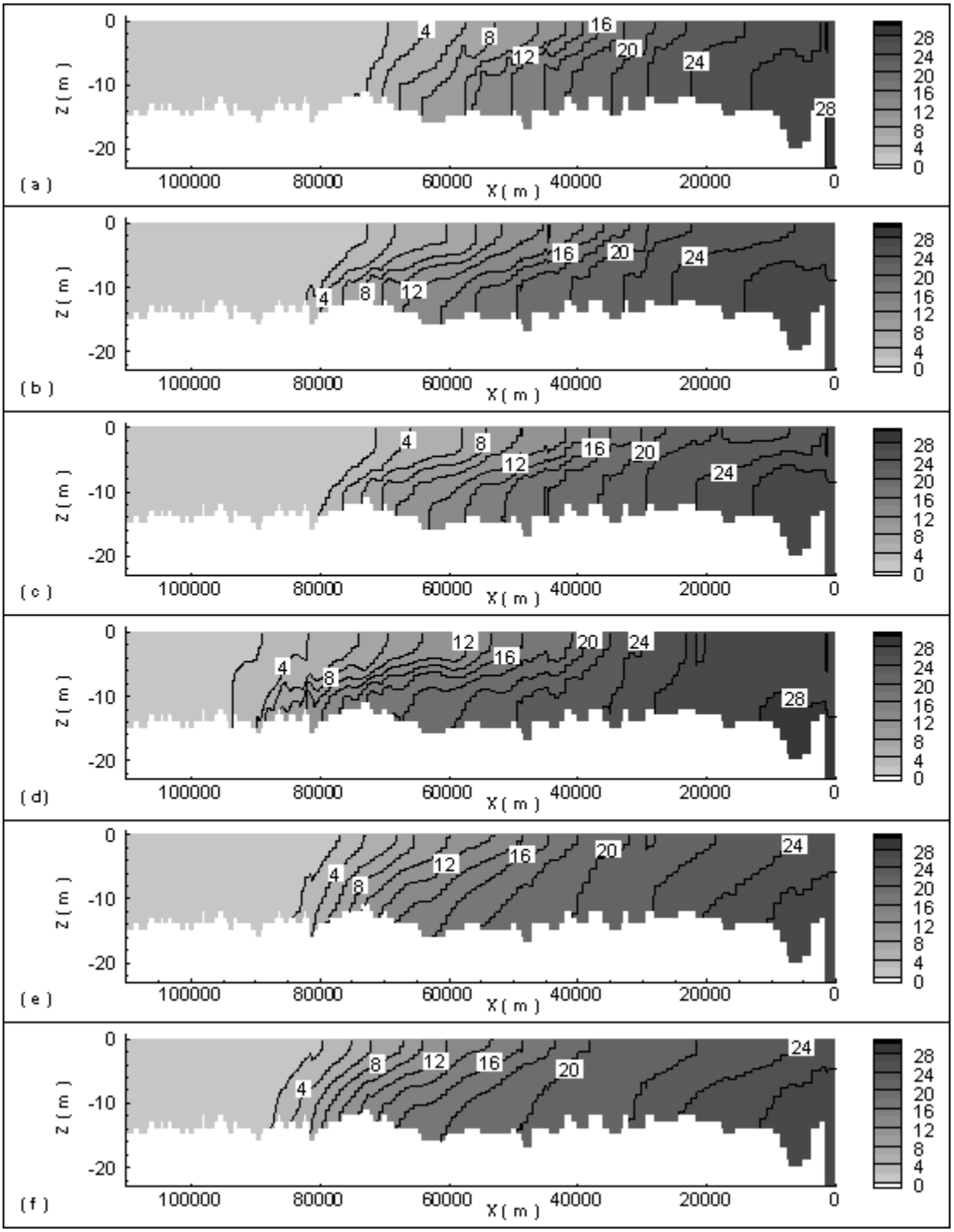

Figure 7. Salinity profiles along the shipping channel for different closure schemes during an ebb tide a) GLS (*k*-*ε*) b) GLS (*k*-*kl*) c) MY25 d) GLS (*k*-*ω*) e) Algebraic f) Constant

The *k*-*ε* model has a well mixed bottom layer and then shows a moderate degree of stratification towards the surface layers suggesting larger vertical mixing coefficients. This is also supported by the fact that the tidal variations of salinity amplitudes are smaller than the other models, implicating added viscosity and internal friction.

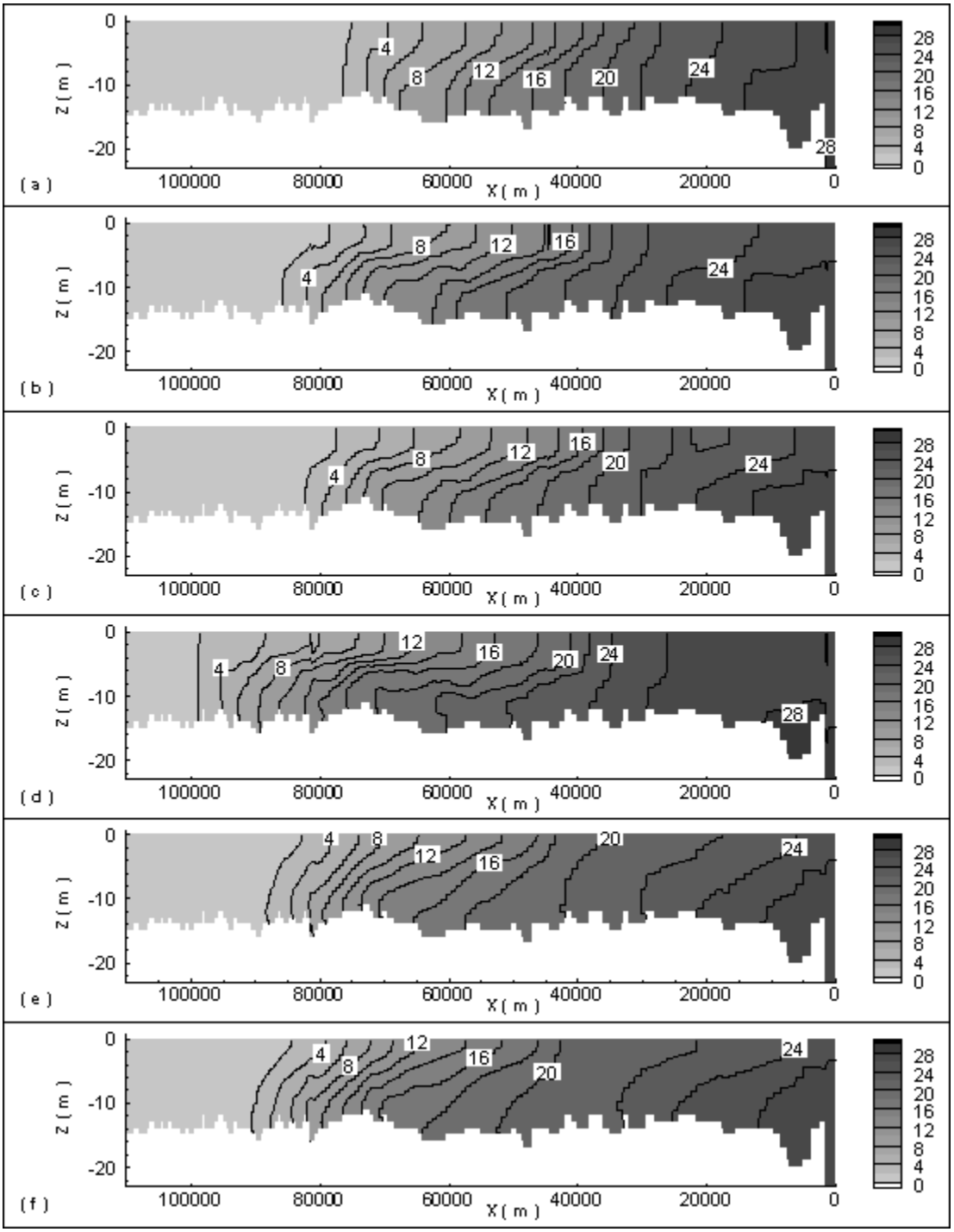

Figure 8. Salinity profiles along the shipping channel for different closure schemes during a flood tide a) GLS (*k-ε*) b) GLS (*k-kl*) c) MY25 d) GLS (*k-ω*) e) Algebraic f) constant

The salinity front (2 psu) for *k-ε* is located at kilometer 78 during flood tide and the variation between the flood and ebb tide is 4 km. The *k-ω* model shows the highest level of stratification around 12psu (Figure 8) and the salinity front is located between kilometers 94-98 for ebb and flood tides.

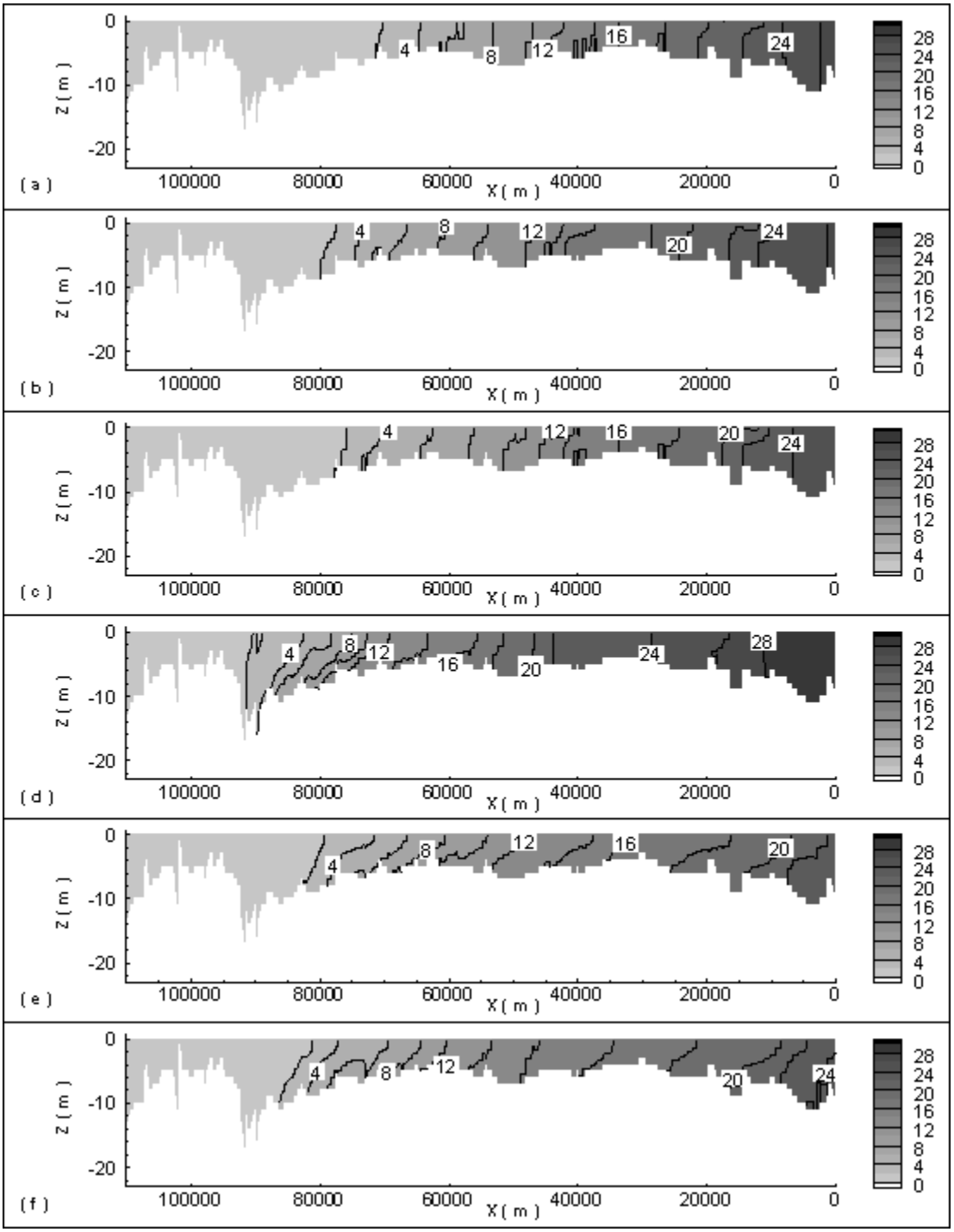

Figure 9. Salinity profiles along a shallow cut shown in Figure 1 for different closure schemes during an ebb tide a) GLS (*k*-*ε*) b) GLS (*k*-*kl*) c) MY25 d) GLS (*k*-*ω*) e) Algebraic f) constant

The salinity front for the *k*-*ε* is located at river kilometer 78 for the flood tide with a range of about 4km between the flood and ebb tide locations. The *k*-*ω* model shows the highest level of stratification with a difference of about 8 psu between bottom and

surface (Figure 8). The salinity front is located between river kilometers 94 and 98 for ebb and flood tides, respectively.

When comparing the *k-kl* (GLS internal Mellor-Yamada) and the separate MY25 model, the salt front of the *k-kl* model migrates 2km further upstream than that of the MY25. The behavior of both models is similar for ebb and flood tides. Upwelling events are observed in the MY25 formulation at the deep channel mouth (Figure 8). When the salinity contours of the main channel and slice 1 are compared, it is seen the shallow parts in the bay are mostly well mixed (Figure 9) in all turbulence closures even though local stratifications due to high bottom slopes are noticeable.

4. Summary and Discussion

The generic length scale turbulence closure is implemented into the UnTRIM numerical model. Different turbulence closure models are applied to the Delaware Bay for a simulation period of two months in July-August, 2003. All simulations are performed with identical boundary conditions and none of the models are calibrated to fit the available data. The available data is based on a salinity time series available at a single station in the middle of the estuary. This is a somewhat limited data base, and the content of our discussions must be seen in the light of this sparse data set. Yet, it provides a basis that allows a first assessment how different the closure schemes perform. There are several outcomes from the test runs.

All of the models simulated the water surface elevations with reasonable accuracy, some more closely (*k-ω*, *k-kl*) others a little less accurate (*k- ε*), but still within acceptable bounds. This indicates that the effect of vertical mixing on water surface elevation is smaller compared to the tidal forcing. UnTRIM model accurately simulated the hydrodynamic system with specified boundary conditions and inflow values.

Low order models such as constant viscosity approach and mixing length theory do not produce satisfactory results for salt transport, i.e. they show significant deviations from the measured salinity data. The mean amplitudes also deviate from the available data for these models. This suggests that the use of more complex approaches than low order closures are needed to better characterize the nature of turbulence. The GLS (*k-ω*) model showed the furthest salinity intrusion and also did not match the available data, even though to a better degree than the low order approaches. The GLS (*k-kl*) closure reproduced the results of the Mellor-Yamada level 2.5 model within reasonable accuracy and can be considered equivalent in their level of performance. Both methods performed better than the GLS (*k-ω*) approach closely following the rising and falling trends in the mean salinity even though the mean values are slightly overestimated. Although showing the smallest degree of upstream salinity migration, the GLS (*k-ε*) model matched the available sensor data best for the Delaware Bay.

From the present investigation, one can conclude that: i) lower turbulence models do not perform adequately (though not terribly wrong) in the Delaware Bay prompting the suggestion to use a 2-equation closure approach, ii) that the GLS (k- ε) approach appeared to best match the available salinity data, even though performing slightly less accurate when predicting water level elevations, and iii) that various closure models yield substantially different results. When compared to the other three two-equation models, the difference, in our opinion, is significant enough to warrant an educated selection, rather than randomly choosing any of the models. In this case the GLS (k- ε) approach appears to work best, even though it is difficult to discern general rules for the selection of an appropriate or the best model for other modeling domains. There is a good chance that any of the closure models might work better for a different estuary, which would suggest that any modeler might want to consider a test-scenario with which to test and compare different closure models first, before settling for the final choice.

References

Burchard, H. (2002). *Applied turbulence modelling in marine waters.* Springer, Berlin; New York.

Casulli, V. (1990). "Semi-Implicit Finite-Difference Methods for the 2-Dimensional Shallow-Water Equations." *Journal of Computational Physics,* 86(1), 56-74.

Casulli, V., and Walters, R. A. (2000). "An unstructured grid, three-dimensional model based on the shallow water equations." *Int.J.Numer.Methods Fluids,* 32(3), 331-348.

Casulli, V., and Zanolli, P. (2005). "High resolution methods for multidimensional advection-diffusion problems in free-surface hydrodynamics." *Ocean Modelling,* 10(1-2), 137-151.

Casulli, V., and Zanolli, P. (2002). "Semi-implicit numerical modeling of nonhydrostatic free-surface flows for environmental problems." *Math.Comput.Model.,* 36(9-10), 1131-1149.

Celebioglu, T. K., and Piasecki, M. (2004). "Addressing design issues of an orthogonal unstructured grid using the grid generator JANET demonstrated on the Delaware estuary." *Estuarine and Coastal Modeling - Proceedings of the Eighth International Conference, Nov 3-5 2003,* American Society of Civil Engineers, Monterey, CA, United States, 1044-1053.

Cook, T. L. (2004). "Observations of Sediment Transport in the Delaware Estuary During Spring Runoff conditions." Ms. thesis, University of Delaware, Delaware.

Garvine, R. W., Mccarthy, R. K., and Wong, K. C. (1992). "The Axial Salinity Distribution in the Delaware Estuary and Its Weak Response to River Discharge." *Estuarine Coastal and Shelf Science,* 35(2), 157-165.

Hess, K. W. (2002). "Spatial interpolation of tidal data in irregularly-shaped coastal regions by numerical solution of Laplace's equation." *Estuarine Coastal and Shelf Science,* 54(2), 175-192.

Kantha, L. H., and Clayson, C. A. (1994). "An Improved Mixed-Layer Model for Geophysical Applications." *Journal of Geophysical Research-Oceans,* 99(C12), 25235-25266.

Mellor, G. L. (1982). "Development of a Turbulence Closure Model for Geophysical Fluid Problems." *Reviews of Geophysics and Space Physics,* 20(4), 851.

Mukai, A. Y., Westerink, J. J., and Luettich, R. A. (2001). "Guidelines for Using the Eastcoast 2001 Database of Tidal Constituents within the Western North Atlantic Ocean, Gulf of Mexico and Caribbean." *Rep. No. Coastal and Hydraulic Engineering Technical Note CHETN IV-XX,* U.S. Army Engineer Research and Development Center, Vicksburg, MS.

Parker, B., Hess, K., Milbert, D., and Gill, S. (2003). "A national vertical datum transformation tool." *Sea Technol.,* 44(9), 10-15.

Rodi, W. (1987). "Examples of calculation methods for flow and mixing in stratified fluids." *Journal of Geophysical Research,* 92(C5), 5305-5328.

F. Sellerhoff, and Lippert, C. (2005). "JANET (Java Net) grid generator." http://www.smileconsult.de/ (5/1, 2003).

Sommerfield, C. K., and Madsen, J. A. (2003). "Sedimentological and Geophysical survey of the Upper Delaware Estuary." Delaware River Basin Commision, http://www.state.nj.us/drbc/UDelsurvey/index.htm.

Umlauf, L., and Burchard, H. (2003). "A generic length-scale equation for geophysical turbulence models." *J.Mar.Res.,* 61(2), 235-265.

Warner, J. C., Sherwood, C. R., Arango, H. G., and Signell, R. P. (2005). "Performance of four turbulence closure models implemented using a generic length scale method." *Ocean Modelling,* 8(1-2), 81-113.

Wilcox, D. C. (1988). "Reassesment of the scale-determining equation for advanced turbulence models." *AIAA J.,* 26(11), 1299-1310.

Wong, K. C. (1995). "On the Relationship Between Long-Term Salinity Variations and River Discharge in the Middle Reach of the Delaware Estuary." *Journal of Geophysical Research-Oceans,* 100(C10), 20705-20713.

Wong, K. C. (1991). "The Response of the Delaware Estuary to the Combined Forcing from Chesapeake Bay and the Ocean." *Journal of Geophysical Research-Oceans,* 96(C5), 8797-8809.